Symmetry Constraints on Nuclear Quadrupole Resonance Spectra: A Case Study*

Robin L. Armstrong

Department of Physics
University of Toronto
Toronto, Canada
MSS 1A7

Many crystals undergo one or more structural phase changes as their temperature is lowered. Nuclear quadrupole resonance (NQR) spectroscopy provides a sensitive means to detect these transitions, and the observed spectra reflect the change in the symmetry properties of the unit cell. It is of interest to ask how uniquely the symmetry classification of a crystal unit cell at a particular temperature can be identified simply from a consideration of the qualitative features of a NQR spectrum. The present discussion will consider only halogen NQR spectra in crystals for which the high temperature structure is the cubic antifluorite structure, R_2MX_6, and only those transitions which produce structures geometrically related to the cubic antifluorite structure by a continuous distortion. The exercise may be viewed as a specific introduction to the use of group theoretical methods in magnetic resonance.

A NQR spectrum results from magnetic dipole transitions between the allowed energy states caused by the interactions of the nuclear quadrupole moments, $\vec{Q}$, with their local electric field gradients, $\vec{\nabla}E$. Therefore, the spectrum resulting from a particular transition associated with a specific nuclear isotope consists of as many components as there are inequivalent nuclear sites in the unit cell. The relative intensities are proportional to the number of nuclei associated with each of the inequivalent sites.

The cubic antifluorite structure is depicted in Figure 1. Octahedral $[MX_6]^{2-}$ ions are situated at the centers of cubic cages, the corners of which are defined by R^+ ions. The axes of the octahedron are parallel to the cube axes. The six halogen, X, sites in the unit call are equivalent.

Figure 2 shows the ^{35}Cl NQR spectrum of K_2ReCl_6 and the ^{127}I NQR spectrum of Rb_2PtI_6 for the $\pm\frac{1}{2}$ ($\pm 3/2$ transition in the vicinity of structural phase changes which distort the cubic structures. Above the phase transition temperatures, T_c, each spectrum consists of a single line. Below T_c, each spectrum consists of two lines with intensity ratios 2:1. The spectra are, however, qualitatively different. For K_2ReCl_6, the two lines split upward and in an essentially continuous fashion. For Rb_2PtI_6, one line splits upward the other

* The lecture notes are based on an article by R.G.C. McElroy, R.L. Armstrong and M. Sutton. J. Magn. Reson. *38*, 253 (1980).

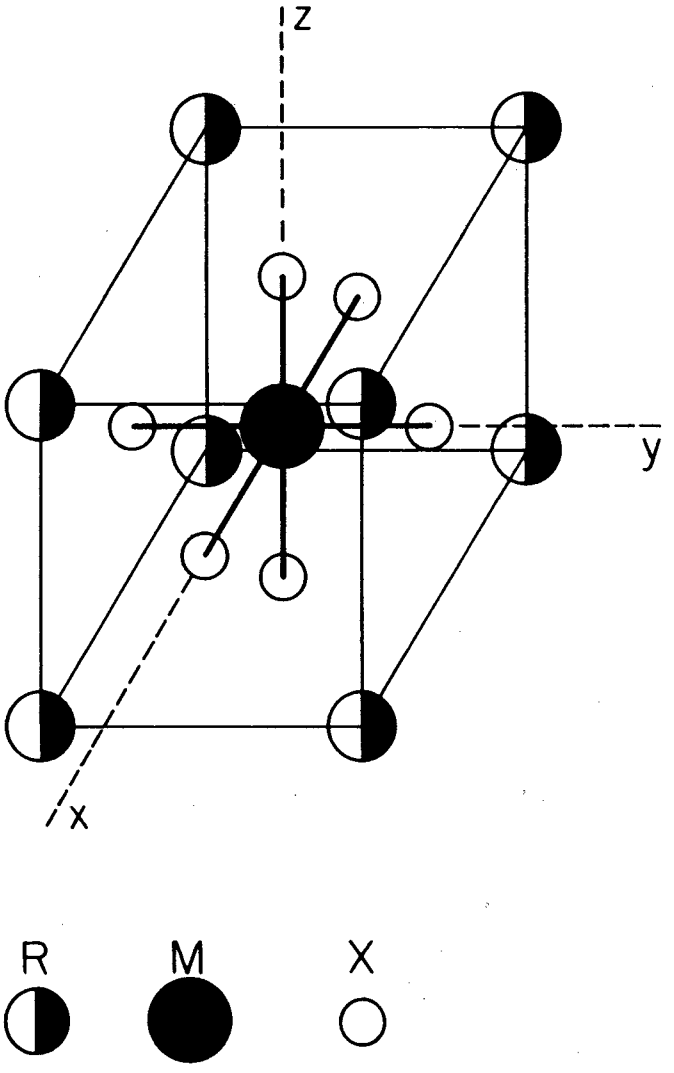

Figure 1. Octahedral $[MX_6]^{2-}$ ions are situated at the centers of cubic cages defined by R^+ ions in the cubic antifluorite structure. The axes of the octahedra are parallel to the cube axes.

downward in such a manner as to approximately conserve the center of mass (intensity-weighted average frequency) of the spectrum through T_c; the splitting occurs in an essentially discontinuous fashion.

The qualitative features of the NQR spectra of the distorted phases of K_2ReCl_6 and Rb_2PtI_6 may be summarized according to the following four criteria:

	Compound	K_2ReCl_6	Rb_2PtI_6
(1)	Number of lines in the spectrum	2	2
(2)	Intensity ratio of the lines	2:1	2:1
(3)	Is the center of mass of the spectrum approximately conserved?	No	Yes
(4)	Is the spectrum essentially continuous across T_c?	Yes	No

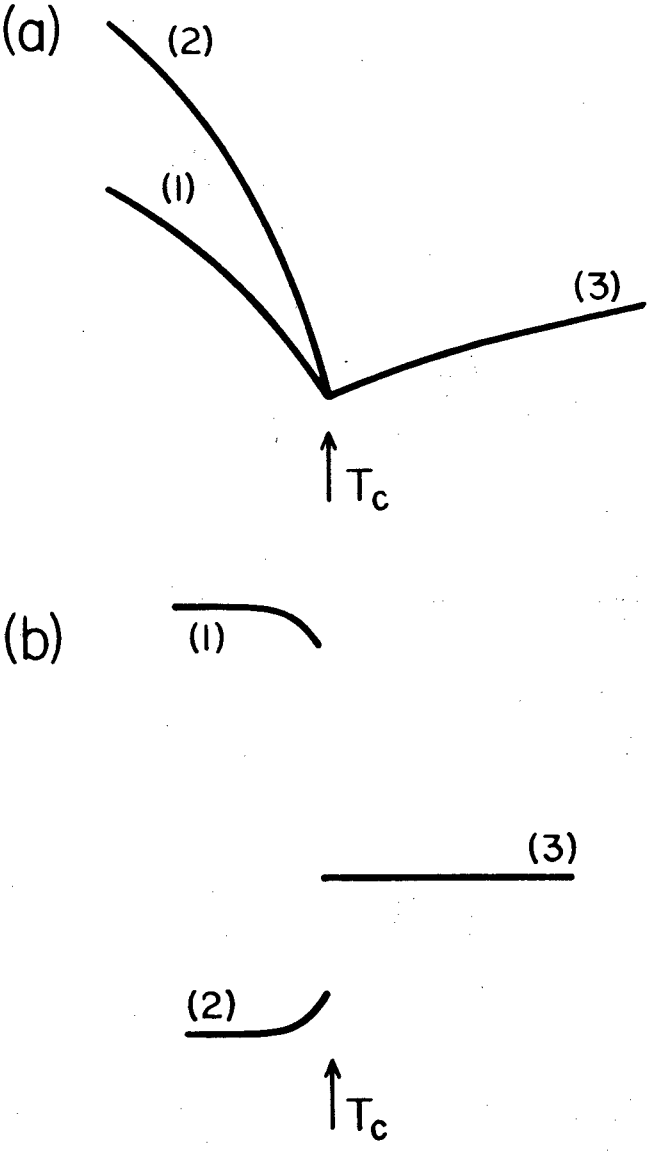

Figure 2. NQR spectra in the vicinity of the structural phase transition that destroys the cubic symmetry. (a) ^{35}Cl spectrum of K_2ReCl_6 (b) ^{127}I spectrum of Rb_2PtI_6 for the $\pm 1/2 \rightarrow \pm 3/2$ transition.

A structural distortion will occur if the displacement pattern associated with a normal mode of vibration of the high temperature structure becomes locked (or frozen) into the low temperature structure. For example, consider a structural distortion resulting from the freezing in of a rotary lattice mode of the antifluorite structure. The displacement pattern for an $[MX_6]^{2-}$ ion for a rotary lattice mode excitation is shown in Figure 3(a). If this pattern becomes locked in below T_c, the equilibrium position of the $[MX_6]^{2-}$ ion is rotated away from its position in the cubic phase, as indicated in Figure 3(b).

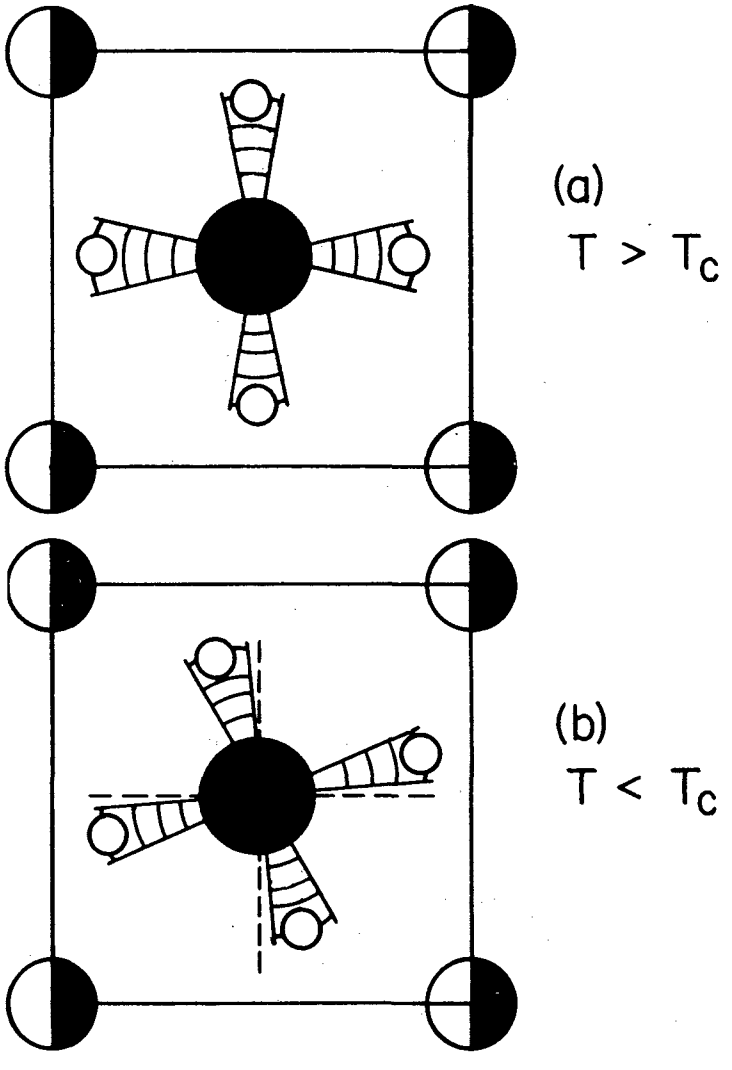

Figure 3. (a) Displacement pattern for a rotary lattice mode excitation above T_c. (b) Freezing in of a rotary lattice mode below T_c causes a static displacement of the equilibrium orientation of the $[MX_6]^{2-}$ ion.

From Figure 3, it is evident that the symmetry of the crystalline environment of the halogen nuclei is reduced as a result of the phase transition. In the high temperature phase, all six X ions are equivalent and experience the same electric field gradient, $\vec{\nabla}E$, so that a one-line NQR spectrum is anticipated. In the low temperature phase, the four X ions in the plane of the page are equivalent and experience a field gradient $\vec{\nabla}E_1$, but the two X ions above and below the page now experience a different field gradient $\vec{\nabla}E_2$. That is, a two-line spectrum with a 2:1 intensity ratio is anticipated.

We now consider the symmetry of the high temperature structure and begin with the symmetry of a cube. The symmetry elements, as indicated in Figure 4, are:

i) the identity
ii) three four-fold rotation axes
iii) four three-fold rotation axes
iv) six two-fold rotation axes
v) inversion center

Associated with these 15 symmetry elements are 48 distinct symmetry (or covering) operations. These are listed below:

i) E: identity or do-nothing operation.
ii) C_4^1, C_4^2, C_4^3: rotations of $\pi/2$, π, $3\pi/2$ about a C_4 axis; there are nine such elements since there are three four-fold axes.
iii) C_3^1, C_3^2: rotations of $2\pi/3$, $4\pi/3$ about a C_3 axis; there are eight such elements since there are four three-fold axes.
iv) C_2^1: rotation of π about a C_2 axis; there are six such elements since there are six two-fold axes.
v) i: inversion operation, the replacement of x by $-x$, y by $-y$, z by $-z$.
vi) C_4^1 X i, C_4^2 X i, C_4^3 X i: inversion operation followed by rotations of $\pi/2$, π, $3\pi/2$ about a C_4 axis; there are nine such elements.
vii) C_3^1 X i, C_3^2 X i: inversion operation followed by rotation of $2\pi/3$ about a C_3 axis; there are eight such elements.
viii) C_2^1 X i: inversion operation followed by a rotation of π about a C_2 axis; there are six such elements.

Each covering operation can be related to a particular permutation of the numbers 1 to 8 which may be associated with the eight corners of the cube. Some examples are shown in Figure 5.

These forty-eight symmetry operations constitute a group in the mathematical sense. That is, a *group*

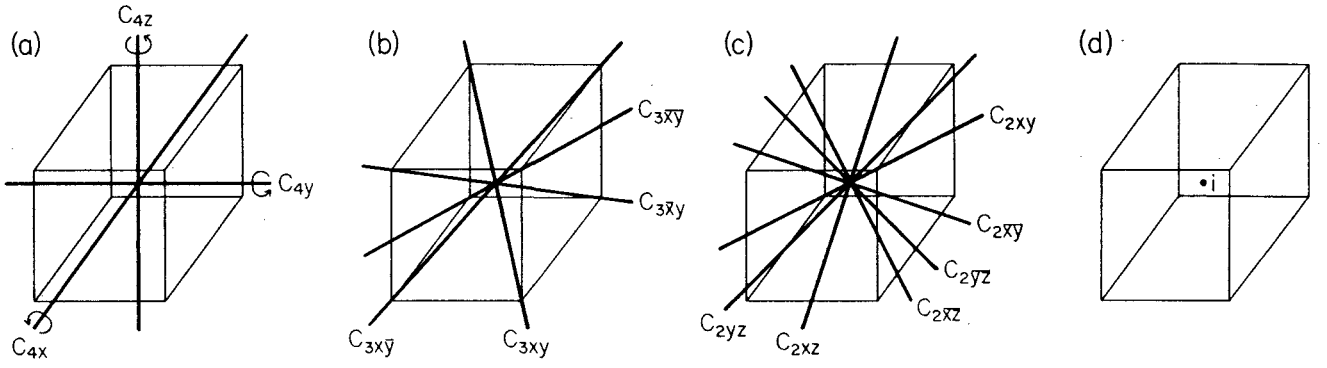

Figure 4. The symmetry elements of a cube (a) Three C_4 axes (b) Four C_3 axes (c) Six C_2 axes (d) Inversion center.

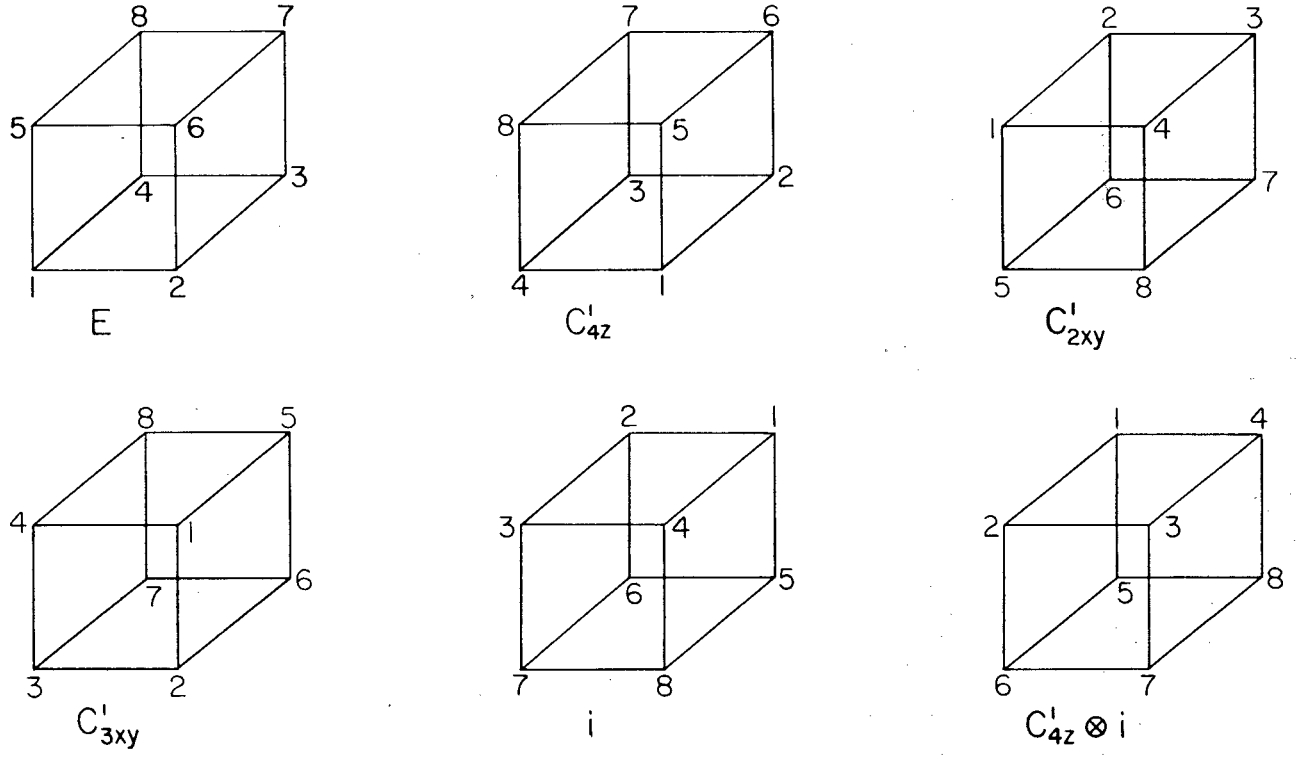

Figure 5. Six examples of the relations between the covering operations of a cube and the permutation operations on the numbers 1 to 8.

multiplication law exists and satisfies certain requirements. We identify the multiplication of two symmetry operations R_i and R_j by the symbol $R_i \times R_j \equiv R_i R_j$ and we mean that the operations are to be carried out consecutively, R_j followed by R_i. The requirements that the set of operations $\{R_i\}$ constitute a mathematical group are as follows:

i) The product operation R_iR_j is equivalent to a single operation R_k which belongs to the set; that is, the set of operations $\{R_i\}$ is closed under the law of group multiplication.

ii) The associative law holds; that is, $R_i(R_jR_k) \equiv (R_iR_j)R_k$.

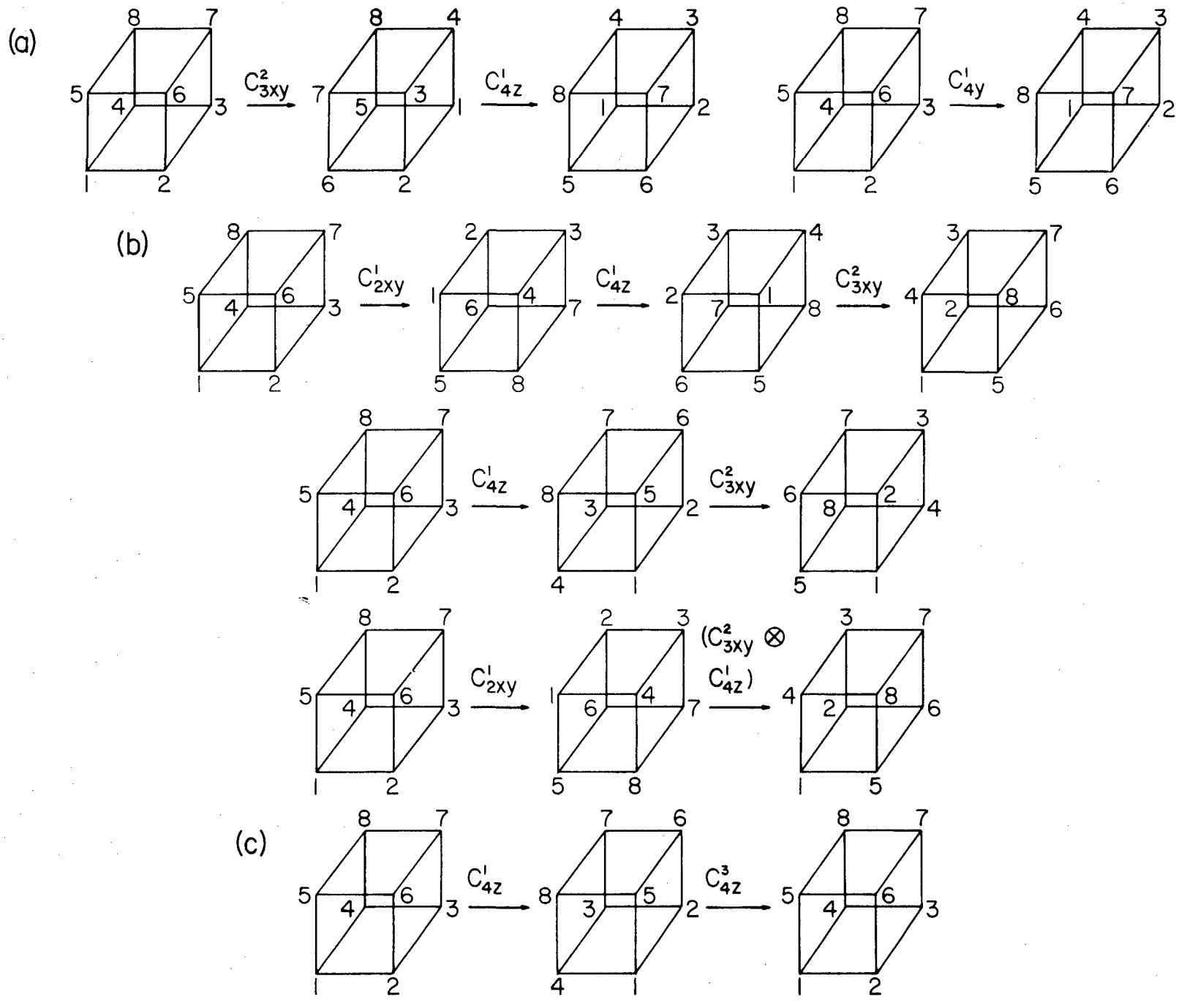

Figure 6. Explicit demonstrations of group multiplication laws. (a) $C^1_{4z}\, C^2_{3xy} = C^1_{4y}$ (b) $C^2_{3xy}\,(C^1_{4z}\, C^1_{2xy} = (C^2_{3xy}\, C^1_{4z})\, C^1_{2xy}$ (c) $C^3_{4z} = (C_{4z})^{-1}$

iii) There is an identity operation E such that $ER_i = R_iE = R_i$.

iv) There corresponds to each operation R_i an inverse operation R_i^{-1} such that $R_iR_j^{-1} = R_i^{-1}R_i = E$.

It is instructive to check these laws explicitly for a few specific cases. In Figure 6(a) we show that

$$C_{4z}^1 C_{3xy}^2 = C_{4y}^1$$

as an example of the validity of law (i). In Figure 6(b) we illustrate that

$$C_{3xy}^2 (C_{4x}^1 C_{2xy}^1) = (C_{3xy}^2 C_{4z}^1) C_{2xy}^1$$

as an example of the validity of law (ii). In Figure 6(c) we demonstrate that

$$C_{4z}^3 = (C_{4z}^1)^{-1}$$

as an example of the validity of law (iv).

Placing an octahedron in the cube and orienting it so that its axes are parallel to the axes of the cube does not alter the list of symmetry elements or operations mentioned in the foregoing discussion. Therefore, we have identified the symmetry of the unit cell of the high temperature structure as that of the point group O_h.

Now consider the symmetry of the low temperature structure. All but eight of the symmetry operations are lost. Assuming that the octahedron rotates about the *z*-axis as indicated in Figure 7, the eight remaining symmetry operations are

$$E, C_{4z}^1, C_{4z}^2, C_{4z}^3, i, C_{4z}^1 X i, C_{4z}^2 X i, C_{4z}^3 X i$$

In this case it is essential to include the octahedron in the discussion because it is the displacement of the octahedron relative to the cube that is responsible for the reduction of the overall symmetry.

It is easy to verify that these eight symmetry operations by themselves satisfy the requirements of a mathematical group, namely the point group C_{4h}. This group is said to be a subgroup of the group O_h—all of the operations in C_{4h} are contained in O_h. A distortion of the cubic antifluorite structure resulting from a freezing in the rotary lattice mode produces a structure having a unit cell whose symmetry operations form a subgroup of the group of symmetry operations of the unit cell of the undistorted structure.

If we consider the operations of O_h more closely we see that another of its subgroups, D_{4h}, contains the sixteen operations that would remain following a tetragonal distortion of a cube along one of its principal axes. Such a distortion would be produced by an appropriate homogeneous elastic strain of the crystal. Figure 8 shows a cube that has been stretched along the direction of the *z*-axis. The symmetry operations are

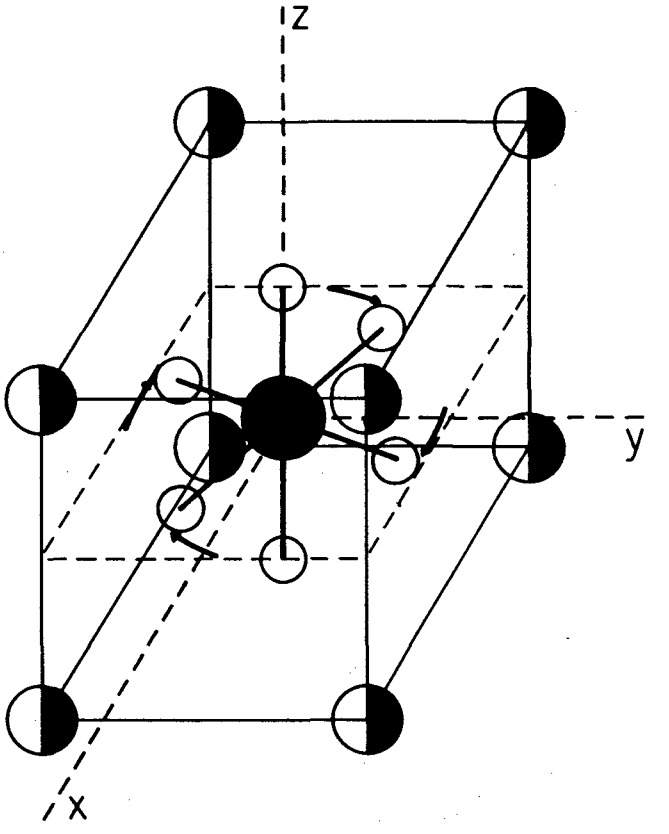

Figure 7. The MX_6 octahedron rotated about the *z*-axis relative to its orientation in the cubic structure shown in Figure 1.

$$E, C_{4z}^1, C_{4z}^2, C_{4z}^3, C_{2x}^1, C_{2y}^1, C_{2xy}^1, C_{2xy}^1, i,$$
$$C_{4z}^1, X i \ldots C_{2xy}^2 X i$$

Note that $C_{2x}^1 \equiv C_{4x}^2$, $C_{2y}^1 \equiv C_{4y}^2$. The two four-fold axes C_{4x}, C_{4y} have become two-fold axes C_{2x}, C_{2y} under the distortion.

For the antifluorite structure, we must assume that a tetragonal distortion of the cage is accompanied by a tetragonal distortion of the octahedron within it, since such an additional distortion does not further reduce the overall symmetry of the unit cell. A tetragonal distortion precipitated by a homogeneous elastic strain could represent a second possible type of structural phase transition for a cubic antifluorite crystal.

A further consideration of the above symmetry operations reveals that the point group C_{4h} is a subgroup of the group D_{4h}. Therefore, if a distortion

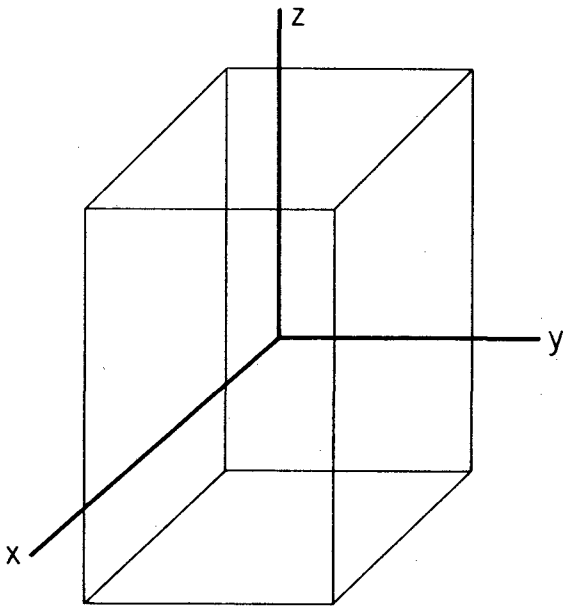

Figure 8. A cube stretched along the direction of the *z*-axis.

of the cubic antifluorite structure occurs as the result of the freezing in of a rotary lattice mode, symmetry considerations do not preclude an associated and spontaneous tetragonal distortion of the lattice. The reverse is, however, not true. A distortion precipitated by a homogeneous strain does not reduce the overall symmetry sufficiently to simultaneously permit a static rotation of the $[MX_6]^{2-}$ octahedral ion.

By moving from the point group of the unit cell of the cubic antifluorite structure through a consideration of the various group-subgroup relations and the possible distortions precipitated by the freezing in of normal mode displacement patterns or the spontaneous occurrence of elastic deformations, a useful hierarchy of point groups can be constructed. From the specific examples discussed here we have developed a portion of that hierarchy:

$$O_h \rightarrow D_{4h} \rightarrow C_{4h}$$

under a homogeneous elastic tetragonal distortion followed by a freezing in of the rotary lattice mode. In Figure 9 a complete hierarchy of point groups relevant to the antifluorite structure is indicated. For each step to a lower symmetry structure along any path, one additional structural parameter is required.

Now we turn to the problem of the determination of expressions for the NQR frequency shifts associated with the various distortions. First consider the distortion from O_h to D_{4h}. This distortion, shown in Figure 10(a), can be represented by a parameter δ which is the increase in the unit cell size along the *z*-axis. Assuming that the distortion preserves the volume of the unit cell, the cell dimensions in the *x*- and *y*-directions will decrease by $\delta/2$. The four X nuclei in the *xy* plane will each experience an identical electric field gradient but a different one from that seen by the two X nuclei on the *z*-axis. To first order in the distortion

$$\Delta\nu_z = {}_o\alpha\delta$$
$$\Delta\nu_{x,y} = -\nu_o\alpha\delta/2$$

The result is a two-line spectrum with intensities in the ratio 2:1. Figure 10(b) shows the case for α positive, as for a point-charge model with the cage only undergoing a tetragonal distortion. Note that

$$\Delta\nu_x + \Delta\nu_y + \Delta\nu_z = 0$$

This states that the center of mass of the spectrum is conserved through the transition. The result does *not* follow from symmetry considerations alone but requires the additional assumptions that the distortion preserves the volume of the unit cell and that the expansion need only be taken to first order in δ.

For the distortion from O_h to C_{4h}, the appropriate expansion parameter is θ, the angle of relative rotation of the octahedron about the *z*-axis as indicated in Figure 11(a). Once again the four X nuclei in the *xy* plane will experience identical field gradients, but different ones from those seen by the two X nuclei on the *z*-axis. To lowest order in the distortion

$$\Delta\nu_z = \nu_o\alpha\theta^2$$
$$\Delta\nu_{x,y} = \nu_o\beta\theta^2$$

For a point charge model with no accompanying tetragonal distortion, α = O and β is positive. The spectrum is shown in Figure 11(b). Note that there is no term linear in θ since a rotation by $-\theta$ is equivalent to a rotation by $+\theta$. If a tetragonal distortion is added,

$$\Psi\nu_z = \nu_o(\alpha\theta^2 + \gamma\delta)$$
$$\Psi\nu_{x,y} = \nu_o(\beta\theta^2 - \gamma\delta/_2)$$

In this case, the center of mass of the spectrum is not conserved through the transition.

A comparison of the predicted spectra with the halogen NQR experimental observations for Rb_2PtI_6 and K_2ReCl_6 as depicted in Figure 2 suggests in the former case a D_{4h} distortion and in the latter a C_{4h} distortion. This identification has been confirmed by X-ray and neutron scattering experiments which yielded the following values for the distortion parameters:

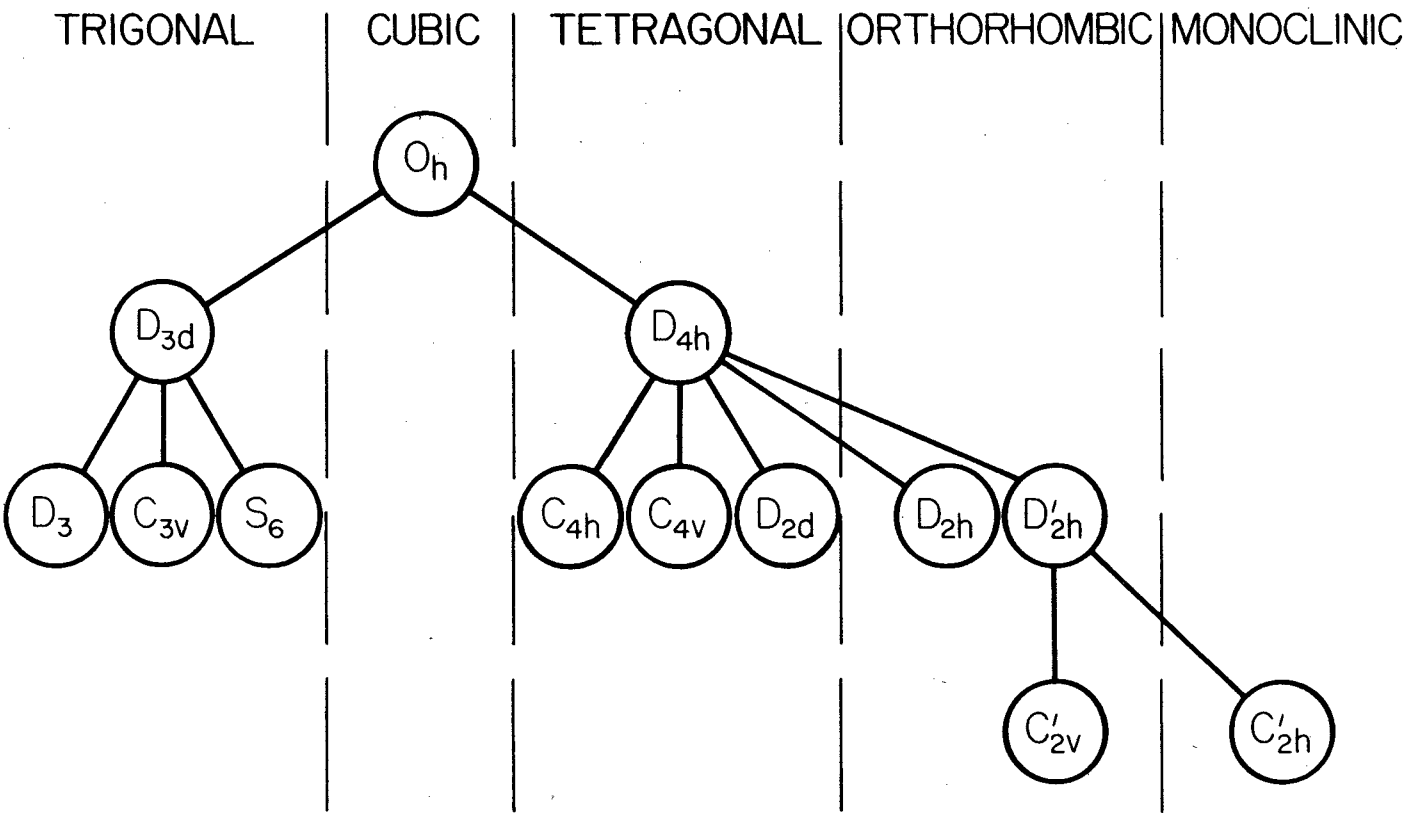

Figure 9. A complete hierarchy of point groups relevant to the antifluorite structure. Since two physically distinct distortions result in the point group D_{2h}, a prime has been added to one group to distinguish between them.

Rb_2PtI_6 $\quad \delta = 0.02a$

K_2ReCl_6 $\quad \theta = 3°, \delta = 0.003a$

Considerations of the various distorted unit cells as described by the subgroups of the group O_h permit expressions for the associated halogen NQR frequency shifts to be obtained. From these formulae can be deduced the number of lines in the NQR spectra, the intensity ratios of the lines, and the conservation or non-conservation of the centers of mass of the spectra through the transition. The specific examples considered lead to spectra having the qualitative features observed for two real crystals, RB_2PtI_6 and K_2ReCl_6.

This completes the discussion of the first three qualitative features of the halogen NQR spectra noted at the beginning of this article. What about the fourth characteristic, the continuity or discontinuity of the spectra at the transition temperature? To answer this question, we consider the form of the free energy of the crystal expanded in terms of the appropriate distortion parameter. In Figure 12(a) we show the form of the free energy for several temperatures assuming that there is no cubic term in the expansion. For a C_{4h} distortion dominated by the rotation of the octahedron, the replacement of θ by $-\theta$ does not alter the free energy. Therefore, there can be no cubic term in the free energy expansion and the transition can occur continuously. Figure 12(b) shows the form of the free energy for several temperatures assuming that there is a cubic term in the expansion. For a D_{4h} distortion, the replacement of δ by $-\delta$ results in a physically different situation and a modified free energy. Therefore, a cubic term occurs in the free energy expansion and the transition must occur discontinuously.

Standard group theoretical methods reveal which normal mode displacement patterns give rise to cubic invariants under the group operations and, therefore, wnich free energy expansions do not contain cubic terms, and hence which modes can precipitate continuous phase transitions. Our considerations have shown that the transition in K_2ReCl_6

can occur continuously, whereas the transition in Rb_2PtI_6 must occur discontinuously. The experimental spectra shown in Figure 2 agree with this prediction.

We have now seen that a relation exists between the qualitative features of the NQR spectrum of the X nuclei in an antifluorite crystal and the distortion associated with the structural phase transition that destroys the cubic symmetry. But how unique is this relationship? That is, how much can be said about the distorted structure simply from the four qualitative characteristics of the associated NQR spectrum that we have identified? The answer is illustrated in Figure 13. It is clear that the qualitative features of the NQR spectrum of the halogen nuclei for an antifluorite crystal provide an excellent starting point for the identification of the unit cell point group symmetry of the distorted phase.

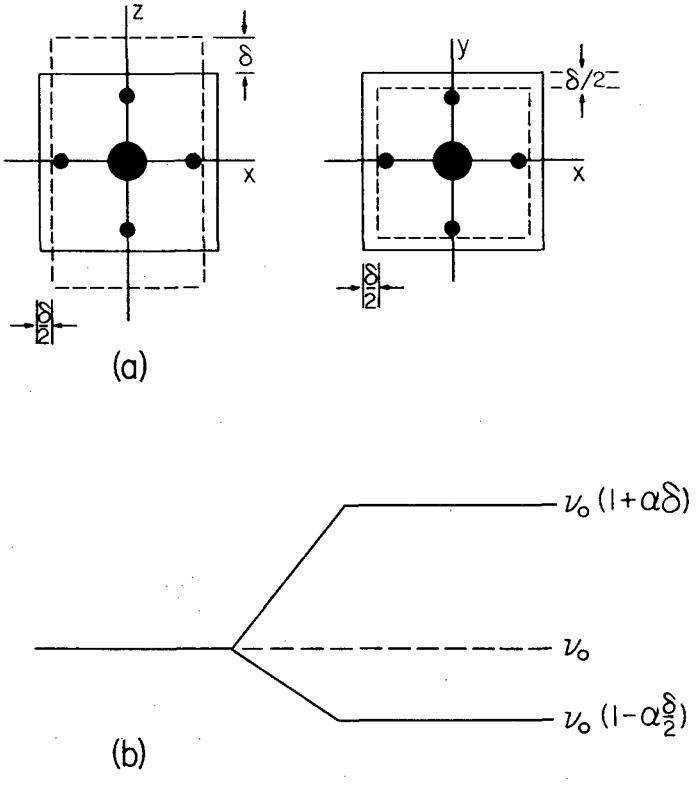

Figure 10. **(a)** The distortion from O_h to D_{4h} can be represented by a parameter δ. **(b)** The two-line spectrum produced by the distortion from O_h to D_{4h}.

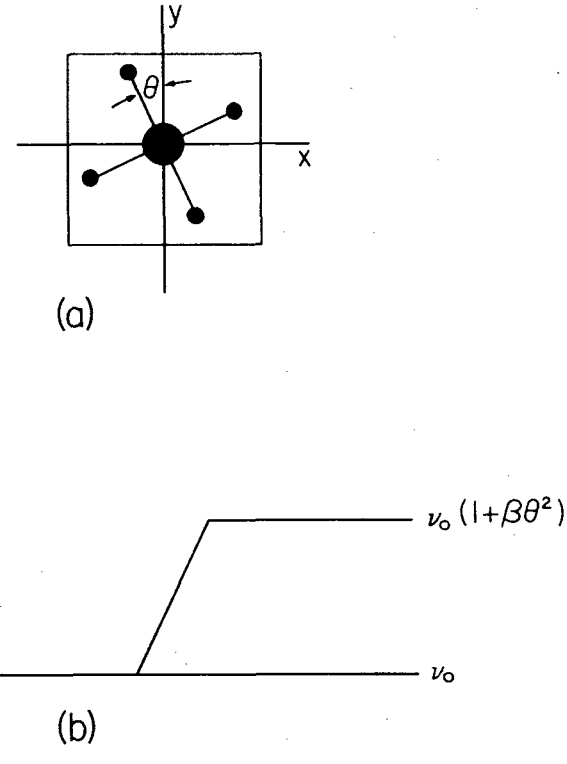

Figure 11. **(a)** The distortion from O_h to C_{4h} can be represented by a parameter θ. **(b)** The two-line spectrum produced by the distortion from O_h to C_{4h}.

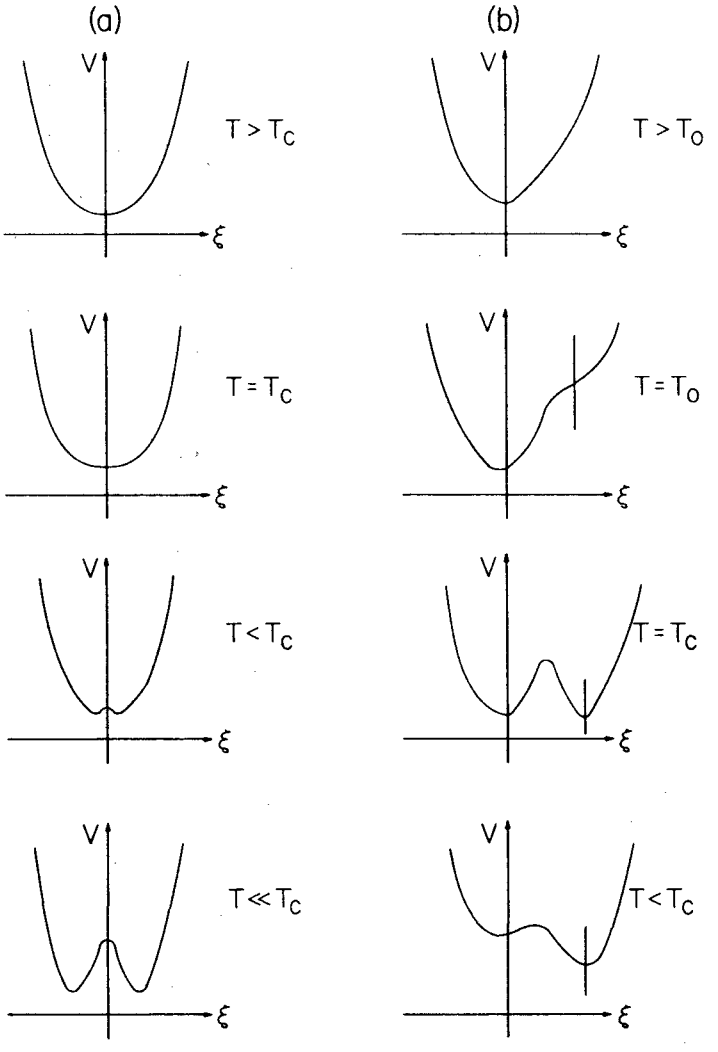

Figure 12. Free energy vs distortion parameter for several temperatures depending on whether a cubic term is assumed in the expansion: **(a)** without cubic term; **(b)** with cubic term.

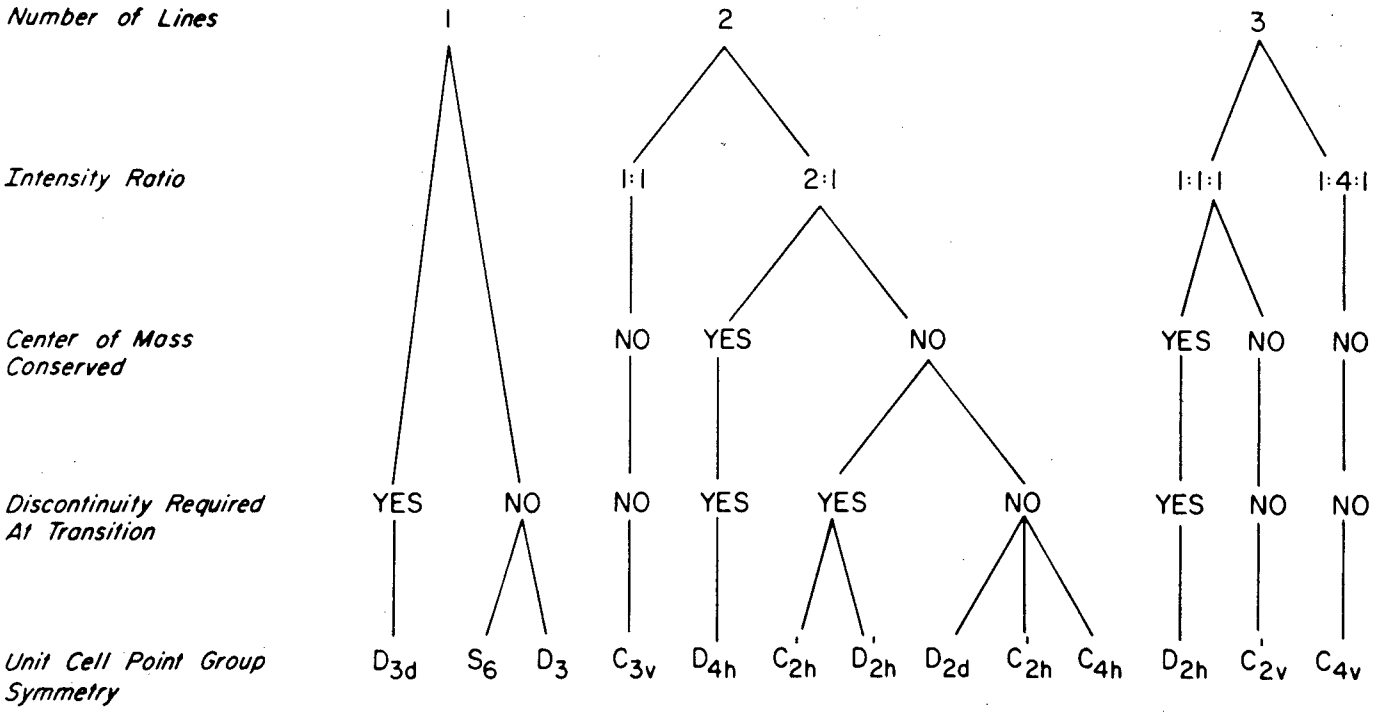

Figure 13. Classification of halogen NQR spectra for antifluorite crystals with respect to four readily observable characteristics.